Nuclear Instruments and Methods in Physics Research A 740 (2014) 117–123

Contents lists available at ScienceDirect

Nuclear Instruments and Methods in Physics Research A

journal homepage: www.elsevier.com/locate/nima

2D theory of wakefield amplification by active medium

Miron Voin [a,*], Wayne D. Kimura [b], Levi Schächter [a]

[a] Department of Electrical Engineering Technion—Israel Institute of Technology, Haifa 32000, Israel
[b] STI Optronics, Inc. 2755 Northup Way, Bellevue, Washington 98004, USA

ARTICLE INFO

Available online 8 November 2013

Keywords:
Gaseous active medium
Stimulated radiation
Laser acceleration

ABSTRACT

A train of microbunches generates in a passive dielectric-loaded waveguide an electromagnetic wake which propagates at the speed of the particles. This wake consists of propagating modes provided the electrons exceed the Cerenkov velocity. If the material is replaced with an active dielectric, identical to that of a laser, the wake is amplified. Another train of bunches, lagging many wavelengths behind, may be accelerated by this amplified wake. The gradient is limited by breakdown and saturation of the medium. Beam loading may be partially or even completely compensated by the gain along the trailing bunch. Preliminary results of a linear theory will be presented, assuming a 300 MeV beam and high-pressure CO_2 mixture as an active medium. In spite of many hundreds of modes excited by the front beam, the spectrum of the amplified field corresponds to a monochromatic wave determined primarily by the bandwidth of the medium. The analytic approach facilitates simple assessment of the effect of the various parameters on the accelerating gradient.

1. Introduction

In the category of structure-less acceleration schemes there are two main conceptual mechanisms which may be divided according to the initial origin of the energy: in one case, an intense laser pulse [1] is injected in a plasma and the particles are accelerated by the trailing space-charge wake. Obviously, the initial energy required for acceleration is stored in the *laser pulse*. In the second paradigm, the laser pulse is replaced by an intense *electron beam* [2,3] as the energy source – the acceleration itself is again facilitated by the emerging space-charge wake. A third possibility, which will be investigated in detail here, is to store the energy within the *medium* and the particles may gain energy at the expense of the latter. The proof of principle experiment of the concept for a structure-less configuration was performed at Brookhaven National Laboratory-Accelerator Test Facility (BNL-ATF) in 2006 [4]. Its essence was to velocity modulate a 45 MeV electron beam by a 0.5 GW CO_2 laser in a wiggler [5]. After 2.5 m drift the velocity-modulated beam emerging from the first module becomes density-modulated and it is injected in a second module which consists of a 30 cm long vessel filled with a CO_2 mixture identical to that of the CO_2 laser. This mixture was kept at 0.25 atm and could be excited by a (30–40 keV) discharge circuit. Comparing the electrons' spectrum with the discharge on and off, a significant fraction (more than 10%) of the electrons gained about 200 keV corresponding to an accelerating gradient of less than 1 MV/m. In the framework of this experiment there was no confining structure that facilitates acceleration, the electrons in the train extract energy from the active medium and the mixture is designed such that no Cerenkov radiation is generated.

In this publication our goal is to present the details of an analysis of a new paradigm whereby all three constraints mentioned above are removed: (i) Rather than energy being transferred from the medium to the same bunch that stimulates the medium, the energy is transferred to the Cerenkov radiation which in turn may be used to accelerate a different train of electron bunches trailing many wavelengths behind. (ii) The active medium is confined in a cylindrical waveguide such that the multiple reflections facilitate a significant enhancement of the wake. In fact, the trailing train of bunches is to be located in the region where the radiation-medium interaction reaches *saturation*. See schematic of the concept in Fig. 1. In the present study, it is tacitly assumed that the active medium is gaseous (CO_2 mixture); however, most arguments hold for a solid-state medium (e.g. Nd:YAG). With one extra condition: since the electrons move in a vacuum channel of radius R surrounded by a solid-state active medium, it is necessary that the exponential decay of the relevant evanescent wave is as small as possible ($2\pi R/\gamma\lambda_0 \ll 1$). For example, in a vacuum tunnel of $R\sim 5$ mm and medium which resonates at 1 μm, the energy of the electrons must be larger than 15 GeV.

2. Model description

For a conceptual description of the paradigm we examine the *wake* generated by a thin charged loop (Q_b) of radius R_σ, located at

* Corresponding author. Tel.: +972 523354159.
E-mail addresses: miron.voin@orbit-cs.com, mironv@tx.technion.ac.il (M. Voin).

0168-9002/$ - see front matter © 2013 Elsevier B.V. All rights reserved.
http://dx.doi.org/10.1016/j.nima.2013.10.089

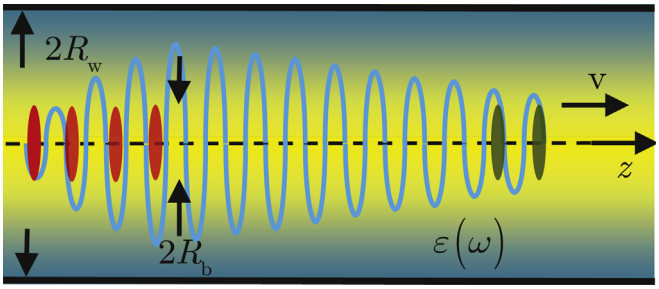

Fig. 1. Schematic of the conceived concept. A trigger bunch generates a weak wake that is amplified by the medium which in turn accelerates a trailing bunch. Beam loading is exaggerated in the drawing. It is shown that it can be compensated by the gain such that the microbunches experience identical acceleration.

$t=0$ at z_σ and as it moves with a velocity v in a waveguide of radius R_w generating a current density

$$J_z(r,z,t) = -Q_b\frac{v}{2\pi r}\delta(r-R_\sigma)\delta(z-z_\sigma-vt) \tag{1}$$

In *vacuum* this loop generates a spectrum of *evanescent* waves. In the framework of our paradigm, we rely on the fact that the same charged-loop moving in a *resonant medium* described by

$$\varepsilon(\omega) = 1+\sum_\nu \omega_{p,\nu}^2/(\omega_{0,\nu}^2+j\omega\Delta\omega_\nu-\omega^2) \tag{2}$$

generates a complex spectrum which contains *propagating* modes and in certain conditions it may lead to an instability that in turn, may result in a *growing wake*. In Eq. (2) $\omega_{0,\nu}$ are the resonances of the medium, $\Delta\omega_\nu$ represents the characteristic bandwidth near each resonance and the "plasma-frequency" will be determined subsequently based on standard laser theory.

The magnetic vector potential associated with the wake is

$$A_z = \frac{Q_b\mu_0}{(2\pi)^2}\sum_s U_s(r)\int_{-\infty}^{\infty} d\omega \frac{\exp(j\omega\tau_\sigma)}{-(p_s/R_w)^2-(\omega/v)^2+\varepsilon(\omega)(\omega/c)^2} \tag{3}$$

where $U_s(r)\equiv J_0(p_s r/R_w)J_0(p_s R_\sigma/R_w)/J_1^2(p_s)(R_w^2/2)$, J_0 is the zero order Bessel function of the first kind, p_s are the zeros of J_0 and $\tau_\sigma\equiv t-(z-z_\sigma)/v$.

In order to envision the characteristics of the spectrum generated by the charged loop in the waveguide, we need to bear in mind that in the presence of the medium the poles associated with Green's function vary, as reflected in the denominator of the integrand of Eq. (3).

In vacuum the poles of the integrand would have pure imaginary values $\omega=\pm jp_s c\beta\gamma/R_w\equiv\pm j\omega_s\beta\gamma$ whereas, in the medium, the poles are a solution of

$$-(p_s/R_w)^2-(\omega/v)^2+\varepsilon(\omega)(\omega/c)^2=0 \tag{4}$$

thus we may get many more poles than in the vacuum case according to various resonances of the dielectric function.

For simplicity sake, we assume a medium to have a *single* active resonance and represent all the passive resonances in the dielectric function [Eq. (2)] by a lossless dielectric coefficient $\varepsilon_r-1>0$ implying,

$$\varepsilon(\omega)\simeq\varepsilon_r+\omega_p^2/(\omega_0^2+j\omega\Delta\omega-\omega^2). \tag{5}$$

Eq. (4) becomes a 4th order polynomial, where two groups ($s=1,2\ldots\infty$) of its zeros being related to evanescent modes and the other two, represent propagating modes

$$(\omega_0^2+j\omega\Delta\omega-\omega^2)[\omega_s^2-(\varepsilon_r-\beta^{-2})\omega^2]=\omega_p^2\omega^2 \tag{6}$$

as revealed by the expressions in the left hand side, whereas the right hand side is responsible for the *coupling* between these two groups of modes.

3. Active medium

Before we proceed to the analysis of the modes, let us consider in more detail the parameters of what may be conceived as a realistic medium. For this estimate we consider the various parameters of the resonant medium based on the proven CO_2 laser systems at BNL [6] and UCLA [7]. Since our goal is to deliver maximum energy to the electrons and based on the experience in the proof of principle experiment performed in 2006 [4] at 0.25 atm, we consider a CO_2 mixture held at higher than standard atmospheric pressure (2.5–10 atm). In addition, we need to have in mind that for accelerating the electron pulse, the electromagnetic energy needs to be drained from the medium on a similar time-scale duration. Ideally, for effectively accelerating a 30 μm long relativistic electron pulse, the energy drained from the medium needs to occur on a time scale of 0.1 ps corresponding to 10 THz bandwidth. As a reference, let us consider a conventional CO_2 laser operating on the 10P vibrational-rotational energy-states at 1 atm. It consists of discrete rotational transitions separated by 55 GHz with a 3.7 GHz bandwidth. According to Ref. [7] for a mixture CO_2:N_2:He (1:1:14), at 25 atm due to the overlap between the various resonances in the manifold, the effective bandwidth exceeds the 1 THz level. However, such a pressure level may prove problematic for our goal.

Beyond the pressure broadening (Δf_p), the electromagnetic field also contributes to the broadening $\Delta\omega_{eff}\simeq\Delta\omega_p+2\Omega_R$ wherein $\Omega_R=\overline{p}E/\hbar$ is the Rabi frequency, E is the local amplitude of the electric field and $\overline{p}$ is the dipole moment associated with the specific transition. This mechanism was the basis of the 3 ps 15 TW CO_2 laser demonstrated at UCLA. In the framework of our linear model, the non-linear process associated with field-broadening is considered in a parametric way.

In the *regenerative amplifier* of the system described in Ref.[6], the small-signal gain with respect to the intensity (at 10 atm) is reported to vary as $2\alpha\sim1$ to 2 m^{-1}. Other sources provide similar results e.g. Ref. [8] $p=10$ atm, $2\alpha\simeq3.5$ m^{-1}; Ref. [9] $p=8$ atm, $2\alpha\simeq2.7$ m^{-1}. For what follows we consider $\alpha=1$ m^{-1}.

We are now in position to correlate this quantity with the "plasma frequency" in Eq. (5) by imposing that at resonance and for a plane wave, the spatial growth rate α which is well known from laser theory [10] is assumed to be equal the spatial growth rate associated with the imaginary component of the wave-vector or explicitly $(\omega_0/c)\mathrm{Im}[\sqrt{\varepsilon(\omega_0)}]=\alpha$ thus

$$\omega_p^2=-2c\alpha\Delta\omega \tag{7}$$

Accordingly, the effective bandwidth (at 10 atm) associated with this pulse is estimated to be 37 GHz thus $\Delta\omega\simeq2\pi\times37$ GHz. Since the parameter of interest, from the interaction perspective, is $\alpha\Delta\omega\simeq2.3\times10^{11}$ m^{-1} s^{-1} we have now established all the quantities that determine Eq. (7). Other gaseous active media have similar characteristics. In this work we are considering a *single* spectral line in the middle of the CO_2 10P branch. Effects of other lines of the same branch as well as effects of other branches will be reported in a subsequent publication.

The relative dielectric coefficient ε_r is determined from dispersion formulas for the refractivity of carbon-dioxide, nitrogen and helium at standard atmospheric pressure and temperature of 273 K provided by Bideau-Mehu [11], Peck [12] and Mansfield [13], respectively. At wavelength of 10.6 μm the estimated ε_r-1 values for CO_2, N_2 and He at 1 atm and temperature of 273 K are 9.4×10^{-4}, 5.9×10^{-4} and 6.9×10^{-5}, respectively. For Nitrogen, an additional verification of the estimated order-of-magnitude value comes from Fenn [14], where at 10 μm, 1 atm and 288 K, the ε_r-1 for dry air is reported as 5.45×10^{-4}. Next we average the ε_r-1 values for the three gases weighed by their partial pressure

at a total pressure of 10 atm and a temperature of 300 K in accordance with the Lorentz–Lorenz equation [15]. In the simulations that follow we use $\varepsilon_r - 1 \simeq 1.42 \times 10^{-3}$. Note that Pantell [16] demonstrated emission of Cherenkov radiation in a gas at atmospheric pressure from a relativistic beam (500 MeV) within the range of our parameters.

4. Spectral analysis

Based on the vector magnetic potential, the longitudinal electric field generated by a charged loop of radius R_σ located at $z = z_\sigma$ at $t=0$ is

$$E_z(r,\tau) = \frac{Q_b}{4\pi\varepsilon_0}\sum_s U_s(r)\frac{1}{\pi}\int_{-\infty}^{\infty} d\omega j\omega F_s(\omega)\exp(j\omega\tau)$$
$$F_s(\omega) \equiv \frac{\varepsilon(\omega)-\beta^{-2}}{\varepsilon(\omega)}\frac{1}{p_s^2c^2/R_w^2 - [\varepsilon(\omega)-\beta^{-2}]\omega^2} \tag{8}$$

For its evaluation in the time-domain we will need to estimate the *poles* associated with the denominator of the last integrand namely the roots of Eq. (6), which may be rewritten by defining the Cherenkov eigen-frequencies $\omega_{C,s}^2 = p_s^2c^2/R_w^2\bar{\varepsilon}$ and the Cherenkov-plasma frequency $\omega_{C,p}^2 = \omega_p^2/\bar{\varepsilon}$ as

$$\omega^4 - (\omega_0^2+\omega_{C,s}^2+\omega_{C,p}^2)\omega^2 + \omega_0^2\omega_{C,s}^2 = j\omega\Delta\omega(\omega^2-\omega_{C,s}^2) \tag{9}$$

where $\bar{\varepsilon} \equiv \varepsilon_r - \beta^{-2}$. This is the *Cherenkov slippage factor* and it will play an important role in what follows. Clearly, for each radial index (s) there are 4 complex solutions one of which may correspond to a growing mode. In the present study we focus on this growing mode. As a starting point is to express the longitudinal electric field [Eq. (8)] in the time domain.

We rewrite the integrand $F_s(\omega)$ such that the poles may be determined in a simple way and ignore the poles associated with the dielectric alone, $\varepsilon(\omega)=0$, hence

$$F_s(\omega) \simeq \frac{1}{\varepsilon_r}\frac{\omega_0^2+j\omega\Delta\omega-\omega^2}{(\omega_{C,s}^2-\omega^2)(\omega_0^2+j\omega\Delta\omega-\omega^2)-\omega_{C,p}^2\omega^2}$$
$$\simeq \frac{A_s/\varepsilon_r}{(j\omega-j\Omega_s)(j\omega+j\Omega_s^*)} + \frac{B_s/\varepsilon_r}{(j\omega-j\Omega_{0,s})(j\omega+j\Omega_{0,s}^*)} \tag{10}$$

This notation distinguishes between the waveguide-like eigen-frequency (Ω_s) and medium-like eigen-frequency (Ω_0). Note that since $F_s(\omega) = F_s^*(-\omega)$ the numerator is real ($A_s = A_s^*$, $B_s = B_s^*$) and Ω_s, Ω_0 are the solutions of the 4th order polynomial and may be approximated

$$\Omega_s = \omega_{C,s} + \delta\omega_s, \quad \Omega_{0,s} = \omega_0 + \delta\omega_{0,s}. \tag{11}$$

Most of the wakes' frequencies are not in resonance with the medium $\omega_{C,s} \neq \omega_0$ therefore the solution is given by

$$\delta\omega_s = \frac{1}{2}\omega_{C,p}^2\frac{\omega_{C,s}}{\omega_{C,s}^2-\omega_0^2-\omega_{C,p}^2-j\omega_{C,s}\Delta\omega}$$
$$\delta\omega_{0,s} = \frac{1}{2}\frac{\omega_0\omega_{C,p}^2 - j\Delta\omega(\omega_{C,s}^2-\omega_0^2)}{\omega_0^2-\omega_{C,s}^2-\omega_{C,p}^2+j\frac{\Delta\omega}{2\omega_0}(\omega_{C,s}^2-3\omega_0^2)}$$
$$A_s = \frac{\Delta\omega/2-\Delta\omega_s}{\Delta\omega_{0,s}-\Delta\omega_s}, \quad B_s = \frac{\Delta\omega_{0,s}-\Delta\omega/2}{\Delta\omega_{0,s}-\Delta\omega_s} \tag{12}$$

wherein $\Delta\omega_s = \mathrm{Im}(\Omega_s)$, $\Delta\omega_{0,s} = \mathrm{Im}(\Omega_{0,s})$. If on the other hand the eigen-frequency of mode $s=s_0$ is in or near resonance with the medium namely, $\omega_{C,s_0} \simeq \omega_0$, then

$$F_s(\omega) \simeq \frac{A_d/\varepsilon_r}{-\omega^2+2j\omega\Delta\omega_{d,+}+\omega_{d,+}^2} + \frac{B_d/\varepsilon_r}{-\omega^2+2j\omega\Delta\omega_{d,-}+\omega_{d,-}^2} \tag{13}$$

wherein

$$\omega_{d,+}^2 \simeq \omega_{d,-}^2 \simeq \omega_0^2$$

$$\Delta\omega_{d,\pm} \simeq \frac{1}{4}(\Delta\omega \pm \sqrt{\Delta\omega^2 - 4\omega_{C,p}^2})$$
$$A_d = \frac{\Delta\omega/2-\Delta\omega_{d,+}}{\Delta\omega_{d,-}-\Delta\omega_{d,+}}, B_d = \frac{\Delta\omega_{d,-}-\Delta\omega/2}{\Delta\omega_{d,-}-\Delta\omega_{d,+}} \tag{14}$$

In the framework of this notation $\Delta\omega$ represents the *full bandwidth* of the active medium spectral line, while $\Delta\omega_{d,+}$ and $\Delta\omega_{d,-}$ represent the *half bandwidth* values for resonances of function $F_s(\omega)$. Comparing the exact and approximated values of $F_s(\omega)$, we find an excellent agreement. With this approximation we may readily evaluate the integral in Eq. (8)

$$G(\tau,\omega_x,\Delta\omega_x) \equiv \frac{1}{2\pi}\int_{-\infty}^{\infty} d\omega \frac{j\omega\exp(j\omega\tau)}{(j\omega)^2+2j\omega\Delta\omega_x+\omega_x^2}$$
$$= \cos(\omega_x\tau)\exp(-\Delta\omega_x\tau)h(\tau) \tag{15}$$

Thus, if $\omega_{C,s_0} \neq \omega_0$

$$E_z(r,\tau) = \frac{Q_b}{2\pi\varepsilon_0\varepsilon_{rs}}\sum_{s\neq s_0} U_s(r)h(\tau)$$
$$\times[A_sG(\tau,\omega_{C,s},\Delta\omega_s) + B_sG(\tau,\omega_0,\Delta\omega_{0,s})] \tag{16}$$

whereas if the mode is close to resonance $\omega_{C,s_0} \simeq \omega_0$ then,

$$E_z(r,\tau) = \frac{Q_b}{2\pi\varepsilon_0\varepsilon_r}U_{s_0}(r)h(\tau)$$
$$\times[A_dG(\tau,\omega_0,\Delta\omega_{d,+}) + B_dG(\tau,\omega_0,\Delta\omega_{d,-})] \tag{17}$$

It is important at this stage to emphasize the major breakthrough associated with our new paradigm. It is incorporated in Eq. (14) which in conjunction with Eq. (7) reveals the growth-rate of the wake that takes the form

$$\Delta\omega_{d,-} \simeq \frac{\Delta\omega}{4}\left(1-\sqrt{1+\frac{8c\alpha}{\Delta\omega\bar{\varepsilon}}}\right) \tag{18}$$

On contrary to the amplification of a wave which is a solution of the *homogeneous* wave-equation (laser) having the form

$$\exp(\alpha z)h(z) \tag{19}$$

in the case of a wake-amplification, corresponding to solution of the *non-homogeneous*wave-equation, the Cherenkov wake is amplified according to

$$\exp[-\tau\Delta\omega_{d,-}]h(\tau) \simeq \exp(\tau c\alpha/\bar{\varepsilon})h(\tau) \tag{20}$$

Clearly, if $\bar{\varepsilon} \ll 1$, then the growth rate may be *orders of magnitude larger* than the spatial growth when the system operates as a laser. In Eq. (20) it was tacitly assumed that $8c\alpha/\Delta\omega\bar{\varepsilon} \ll 1$. At the other extreme, $8c\alpha/\Delta\omega\bar{\varepsilon} \ll 1$,

$$\exp[-\tau\Delta\omega_{d,-}]h(\tau) \simeq \exp(\tau\sqrt{c\alpha\Delta\omega/2\bar{\varepsilon}})h(\tau) \tag{21}$$

and in what follows we consider an intermediate regime $8c\alpha/\Delta\omega\bar{\varepsilon} \sim 10$.

A visualization of this enhanced gain is illustrated in Fig. 2. Top-left frame shows schematically a ray traversing an active medium (α) of length L without reflections, its gain is αL. Once the beam propagates at angle θ (relative to the z-axis), it bounces back and forth between the two reflecting walls and since the effective interaction-length is extended to $L/\cos\theta$ then the effective gain is elevated to $\alpha L/\cos\theta$ – see top-right frame. In the case of Cherenkov radiation, the wake is forced to bounce between the two reflecting walls at the Cherenkov-angle $\cos\theta_{Cer} = 1/\beta\sqrt{\varepsilon_r}$ therefore the gain is $\alpha' L/\sin\theta_{Cer} = \alpha' L\sqrt{\varepsilon_r/\bar{\varepsilon}}$ – see bottom-left frame. Finally, in the bottom-right frame we illustrate the case of a dilute gas $\varepsilon_r \simeq 1$. Clearly, the gain is elevated by Cherenkov slippage term $1/\sqrt{\bar{\varepsilon}}$ namely, $\alpha' L/\sin\theta_{Cer} \simeq \alpha' L/\sqrt{\bar{\varepsilon}}$. In the last three cases, the multiple reflections are responsible for the enhanced effective gain.

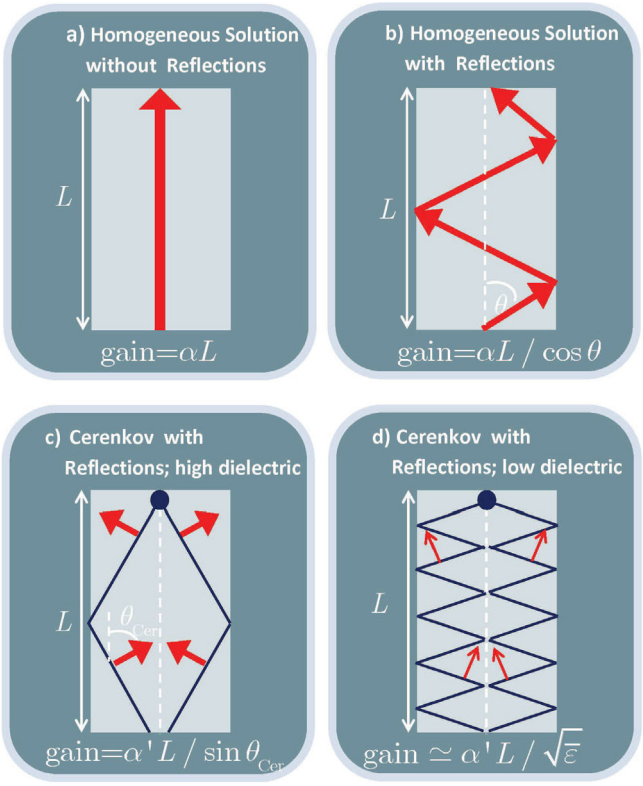

Fig. 2. A visualization of the enhanced gain. Top-left frame (a) shows schematically a ray traversing an active medium (α) of length L without reflections; its gain is αL. In the top-right frame (b), the beam propagates at angle θ relative to the axis of the system; the gain is $\alpha L/\cos\theta$. In the case of Cherenkov radiation, the wake is forced to bounce between the two reflecting walls at the Cherenkov-angle $\cos\theta_{\rm Cer}=1/\beta\varepsilon_{\rm r}^{1/2}$ therefore the gain is $\alpha' L/\sin\theta_{\rm Cer}=\alpha' L(\varepsilon_{\rm r}/\bar{\varepsilon})^{1/2}$ – see frame (c). Finally, in frame (d) we illustrate the case of a dilute gas $\varepsilon_{\rm r}\simeq 1$ thus the gain is $\alpha' L\bar{\varepsilon}^{-1/2}$.

5. Simulation results

Simulation parameters are summarized in Table 1.

Fig. 3 shows the contribution of the various modes at a distance $L=6000\lambda_0$ behind the trigger bunch with the current density given by

$$J_z(r,\tau)=\frac{h(R_{\rm b}-r)}{\pi R_{\rm b}^2}[I_0+I_1\ \cos(\omega_0\tau)]\exp\left[-\left(\frac{\tau}{\Delta t}\right)^2\right] \tag{22}$$

Only one or two modes in the vicinity of resonance have a significant contribution and the remainder are more than 5 orders of magnitude weaker. The inset illustrates off-resonance behavior. While on logarithmic scale the reduction seems modest we will show subsequently that in the time-domain the effect is quite significant.

The enhanced exponential gain is clearly revealed in Fig. 4 where the gradient is illustrated for three cases: $s=s_0=360$, $|s-s_0|\le 160$ and $1\le s\le 1000$; the asymptotic behavior in all three cases is determined by the resonant mode (s_0) while all the others determine the "near-field", adjacent to the trigger bunch. For comparison, if the Cherenkov factor were not present, then at a distance $L=6000\lambda_0$, the gain would have been negligible $\exp(\alpha L)\simeq 1.07$ and not $\exp(|\Delta\omega_{\rm d}|L/c)\sim 10^9$ as the present analysis predicts.

6. Beam loading

We demonstrate now that the exponential gain can solve an inherent problem associated with this paradigm. In today's microwave technology, the *accelerated* bunch generates a wake that tends to reduce the accelerating field. The same phenomenon will occur in our case but here we need a train of microbunches which entails that each microbunch will experience a different gradient. Although small, this variation may be significant over extended acceleration length and therefore, unacceptable. With proper design of the microbunch charges and gain, this effect, in principle, can be eliminated.

Consider a gradient generated by an idealized microbunch of charge q_ν located at $t=0$ and at $z=\zeta_\nu$ is given by

$$E_\nu(\tau)=\frac{q_\nu}{4\pi\varepsilon_0 R_{\rm eff}^2}f\left(\tau+\frac{\zeta_\nu}{\rm v}\right) \tag{23}$$

$R_{\rm eff}$ is a geometric parameter which accounts for the fact that due to linearity of Maxwell equations, the wake is *linear* with the charge which excites it. $f(\tau)\equiv\cos(\omega_0\tau)\exp(\alpha'{\rm v}\tau)h(\tau)$, α' is a parameter proportional to the spatial growth in the medium; $\nu=1,2\ldots$ represents the index of the microbunch. The trigger train of bunches consists of N_T microbunches and for simplicity sake we assume that they all carry an identical charge $Q_{\rm T}/N_{\rm T}$ moreover, they are λ_0 apart namely $\zeta_\nu^{(\rm T)}=-\nu\lambda_0$. In a similar way, the accelerated train consists of $N_{\rm A}$ identical bunches $Q_{\rm A}/N_{\rm A}$ but the

Table 1
Simulation parameters.

Parameter		Value
Medium		
Resonance wavelength (CO_2)	λ_0	10.6 μm
Resonance frequency	ω_0	1.78×10^{14} rad/s
Resonance bandwidth (@ ~ 10 atm)	$\Delta\omega$	2.32×10^{11} rad/s
Growth rate coefficient	α	$1\ {\rm m}^{-1}$
Plasma frequency	$\lvert\omega_{\rm p}\rvert$	1.18×10^{10} rad/s
Relative permittivity	$\varepsilon_{\rm r}$	1.00142
Waveguide		
Radius	$R_{\rm w}$	50.674 mm
Resonance mode	s_0	360
e-beam		
Lorentz factor	γ	600
Total charge	$Q_{\rm total}$	$10^9 e$
Length	$L_{\rm tr}$	$150\lambda_0$
Modulation	$M_{\rm tr}$	20%
Radius	$R_{\rm b}$	4 mm

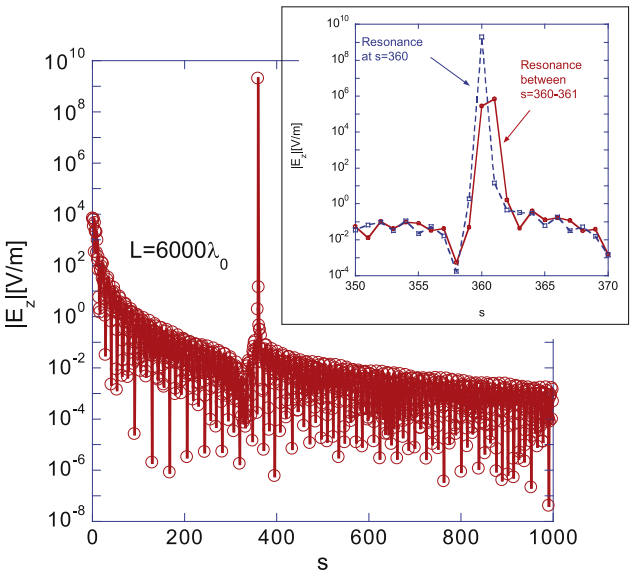

Fig. 3. Contribution of the various modes to E_z. In the inset we compare resonance and off-resonance conditions near the peak.

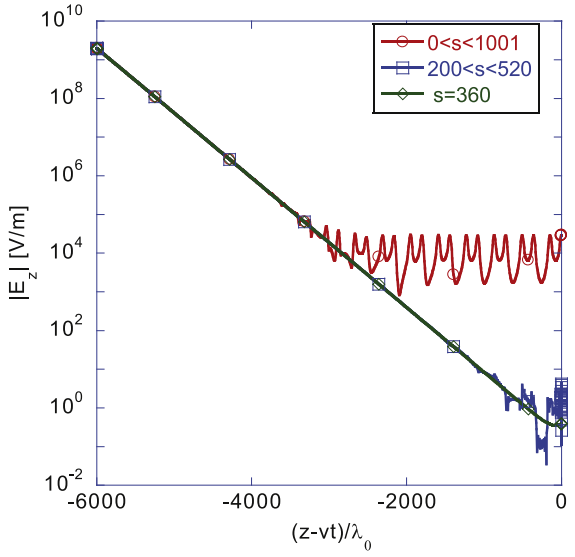

Fig. 4. Amplitude of E_z behind the trigger bunch (time-domain) for three sets of Bessel harmonics: in the first set we consider 1000 modes (red-circles), in the second set we consider 320 modes around the resonant Bessel-harmonic (blue-square). The third set consists of one Bessel-harmonic – the resonant one. Clearly, sufficiently far away from the trigger bunch the resonant mode is dominant. (For interpretation of the references to color in this figure caption, the reader is referred to the web version of this article.)

first one is many wavelengths behind $\zeta_\nu^{(A)} = -(N_{space}+1/2+\nu)\lambda_0$ consequently, the gradient is given by

$$E(\tau) = \frac{Q_T}{4\pi\varepsilon_0 R_{eff}^2}\left\langle f\left(\tau+\frac{\zeta_\nu^{(T)}}{v}\right)\right\rangle + \frac{Q_A}{4\pi\varepsilon_0 R_{eff}^2}\left\langle f\left(\tau+\frac{\zeta_\nu^{(A)}}{v}\right)\right\rangle. \quad (24)$$

Evidently, the gradient along the accelerated train is not uniform as the medium tends to enhance it whereas the beam loading reduces it. Obviously, we need to ensure uniform acceleration for all the electrons and for this purpose we denote by $E_1^{(A)}$ the gradient on the first bunch in the accelerated train. Assuming a point-like microbunch, immediately after the first bunch, this gradient is reduced by $Q_A/4\pi\varepsilon_0 R_{eff}^2 N_A$. The remaining field is amplified by the medium and for achieving uniform acceleration on all microbunches, we impose that at the location of the next microbunch the value of the accelerating gradient is exactly as on the initial microbunch thus

$$(E_1^{(A)} - Q_A/4\pi\varepsilon_0 R_{eff}^2 N_A)\exp(\alpha'\lambda_0) = E_1^{(A)} \quad (25)$$

Having in mind that the gain per period is very small, this condition constraints the spatial growth, the gradient and the charge of a microbunch according to

$$\frac{Q_A}{4\pi\varepsilon_0 R_{eff}^2 N_A}\frac{1}{E_1^{(A)}} = 1-\exp(-\alpha'\lambda_0) \simeq \alpha'\lambda_0 \quad (26)$$

In fact, this condition specifies the ratio of the charge between the two trains since by its own definition,

$$E_1^{(A)} = \frac{Q_T}{4\pi\varepsilon_0 R_{eff}^2}\frac{1}{N_T}\sum_{\nu=1}^{N_T}\exp[\alpha'(\zeta_\nu^{(T)}-\zeta_1^{(A)})]$$
$$= \frac{Q_T}{4\pi\varepsilon_0 R_{eff}^2}\frac{\exp\left[\left(N_{space}+\frac{1}{2}\right)\alpha'\lambda_0\right]}{N_T}\frac{1-\exp(-\alpha'\lambda_0 N_T)}{1-\exp(-\alpha'\lambda_0)} \quad (27)$$

thus, substituting in (26) we get

$$\frac{Q_A}{N_A} = \frac{Q_T}{N_T}\exp\left[\alpha'\lambda_0\left(N_{space}+\frac{1}{2}\right)\right][1-\exp(-\alpha'\lambda_0 N_T)] \quad (28)$$

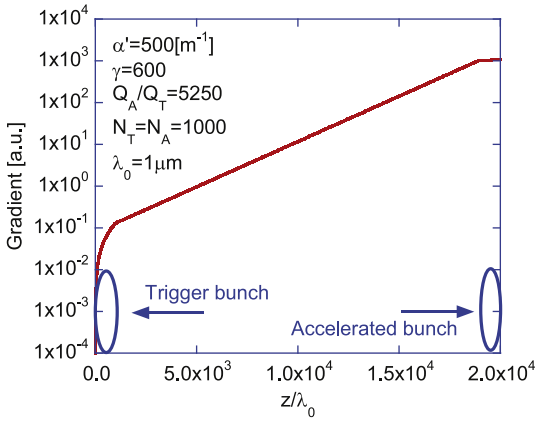

Fig. 5. The trigger bunch generates a wake which is amplified by the medium. If the accelerated train is properly designed and located, the beam-loading may be compensated by the gain.

Note that the larger the gain, the larger the ratio of the charge in the accelerated bunch and the trigger bunch. A typical behavior is illustrated in Fig. 5.

7. Saturation

Being analyzed in the framework of a linear theory, the gain as reflected in the previous section does not account for the medium depletion. A rough assessment of this saturation effect may be developed based on energy conservation and the assumption that the population inversion is *uniform* across the confining waveguide

$$\frac{1}{2}\Delta n(\tau)\hbar\omega_0 + \frac{2}{R_w^2}\int_0^{R_w} dr r\frac{1}{2}\begin{bmatrix}\varepsilon_0 E_r^2(r,\tau)\\ +\varepsilon_0 E_z^2(r,\tau)\\ +\mu_0 H_\phi^2(r,\tau)\end{bmatrix} = \text{const.} \quad (29)$$

The electromagnetic term can be divided in two groups, the resonant harmonic $s = s_0$ and the non-resonant Bessel harmonics $s \neq s_0$ which practically do not interact with the medium and can be ignored. Consequently,

$$\frac{1}{2}\Delta n(\tau)\hbar\omega_0 + J_1^2(p_{s_0})\frac{1}{2}\begin{bmatrix}\varepsilon_0\varepsilon_r E_{r,s_0}^2(\tau)\\ +\varepsilon_0\varepsilon_r E_{z,s_0}^2(\tau)\\ +\mu_0 H_{\phi,s_0}^2(\tau)\end{bmatrix} = \text{const.} \quad (30)$$

and assuming the relation between the field component is similar to the case of passive medium we get

$$\frac{1}{2}\Delta n(\tau)\hbar\omega_0 + \frac{3}{4}\varepsilon_0 J_1^2(p_{s_0})E_{z,s_0}^2(0)\exp(2c\alpha\tau/\bar{\varepsilon})h(\tau) = \text{const.} \quad (31)$$

The growth may be expressed in terms of the population inversion and the cross-section for stimulated emission ($\sigma_{st} \sim 1.5\times 10^{-23}\ m^{-2}$) as $2\alpha = \Delta n\sigma_{st}$, therefore, we may deduce that when the population inversion varies,

$$\frac{1}{2}\Delta n(\tau)\hbar\omega_0 + \frac{3}{4}\varepsilon_0 J_1^2(p_{s_0})E_{z,s_0}^2(0) \quad \times\exp\left\{\frac{2c\sigma_{st}}{\bar{\varepsilon}\hbar\omega_0}\int_0^\tau d\theta\left[\frac{1}{2}\Delta n(\theta)\hbar\omega_0\right]\right\}h(\tau)$$
$$= \frac{1}{2}\Delta n(0)\hbar\omega_0 + \frac{3}{4}\varepsilon_0 J_1^2(p_{s_0})E_{z,s_0}^2(0). \quad (32)$$

Based on the simulations $\bar{\varepsilon} \sim 0.0014$, $E_{z,s_0}(0) \sim 1[V/m]$, $J_1^2(p_{360}) = 5.6\times 10^{-4}$ and since $\alpha = 1 m^{-1}$ we conclude that $\Delta n(0) \sim 1.3\times 10^{23}\ m^{-3}$; $\hbar\omega_0 = 1.88\times 10^{-20}$. It is convenient to use normalized units

$$\bar{n} = \frac{\Delta n(\theta)}{\Delta n(0)}, \quad \bar{\tau} = \frac{1}{\bar{\varepsilon}}\Delta n(0)c\tau\sigma_{st} = \frac{2}{\bar{\varepsilon}}\alpha c\tau,$$

$$\overline{w} = \frac{\frac{3}{4}\varepsilon_0 J_1^2(p_{s_0}) E_{z,s_0}^2(0)}{\frac{1}{2}\Delta n(0)\hbar\omega_0} \sim 3.0\times 10^{-18} \tag{33}$$

which enables us to write Eq. (32) in the form

$$\overline{n}(\overline{\tau}) + \overline{w}\exp\left[\int_0^{\overline{\tau}} d\theta \overline{n}(\theta)\right] = 1+\overline{w}. \tag{34}$$

Rather than its integral form we prefer its differential version

$$\overline{n} = \frac{d}{d\overline{\tau}}\ln\left[\frac{1+\overline{w}-\overline{n}}{\overline{w}}\right] \tag{35}$$

whose solution may be shown to be

$$\overline{n}(\overline{\tau}) = \frac{1+\overline{w}}{1+\overline{w}\exp[\overline{\tau}(1+\overline{w})]} \tag{36}$$

As a reference, let us assume (see Fig. 4) that the amplitude of the resonant mode is $E_0 = 1$ V/m and in time

$$E_z^{(\mathrm{lin})}(\tau) = E_0\exp\left(\frac{1}{2}\overline{\tau}\right)$$
$$E_z^{(\mathrm{sat})}(\tau) = E_0\exp\left\{\frac{1}{2}\int_0^{\overline{\tau}} d\theta\overline{n}(\theta)\right\} = E_0\sqrt{\frac{1+\overline{w}-\overline{n}(\overline{\tau})}{\overline{w}}}. \tag{37}$$

According to the typical values adopted here, the saturation occurs for a gradient of 0.57 GV/m.

8. Discussion

Several tacit assumptions made in the course of this brief analysis need special consideration:

(i) The constitutive relation describing the medium as specified in Eq. (2), has been developed, e.g. [10], from a microscopic dynamic argument (of the atoms) using an electromagnetic field that does not vary across the atom. This tacitly entails that the wavelength of the radiation involved is much longer than the size of the resonant atom ($\lambda_0 \ll a_0 = 0.5\times 10^{-10}$m). Since in our case evanescent waves attached to relativistic particles are also involved, an additional condition may be included $\exp(-2\pi a_0/\gamma\lambda_0)\sim 1$ thus $\gamma\lambda_0 \gg a_0$. Evidently, this condition is weaker than the previous.

(ii) For all relevant media, the effective size of the atom is generally much smaller than the characteristics lengths – with the exception of the classical radius of the electron. This comes into play when we describe the gain α which according to the classical laser theory is expressed in terms of the population inversion (Δn) and the cross-section for stimulated emission (σ_{st}) namely, $2\alpha = \Delta n\sigma_{\mathrm{st}}$ [17, p. 287, (54)]. In most media the latter is not larger than 10^{-22} m^2 making the evanescent waves perfectly equivalent to propagating waves from the perspective of the interaction with the single atom.

(iii) By its own definition, the dielectric function can account only for linear processes, non-linear processes such as field-broadening (Rabi) or reduction of the population inversion can be assessed only as a general trend. Moreover, when assuming that the population inversion is set constant, we practically assume that the energy converted from the medium to the electromagnetic field or the electrons are negligible. In a past publication [18] we considered this loading effect in detail and we showed that the electrons may drain virtually all the energy from the medium. Furthermore, in this context we should point out that typically relevant electron bunches contain of order 10^{10} electrons whereas the number of excited atoms is typically of the order of 10^{20} ($=\Delta n\times$ volume $\sim 10^{23}$ m$^{-3}\times 10^{-3}$ m^3). Consequently, assuming an ideal interaction each electron may absorb 10^{10} photons stored in the medium.

(iv) Eq. (3) indicates that the spectrum of photons (real or virtual) as carried by a bunch of electrons is itself affected by the dielectric function. However, in order to assess the number of virtual photons impinging upon the active medium (assuming finite extent) we may resort to the vacuum solution for the magnetic vector potential, calculate the energy carried by each Bessel-harmonic ($W = \sum_s W_s$). Accordingly, the number of virtual photons at that frequency ($\omega_s = p_s c\beta\gamma/R_{\mathrm{w}}$) carried by a relativistic electron is

$$N_{\mathrm{ph},s}^{(\mathrm{v})}(\gamma\gg 1) = W_s/\hbar\omega_s = \alpha_{\mathrm{F}}/[p_s J_1(p_s)]^2 \tag{38}$$

$\alpha_{\mathrm{F}} = e^2/4\pi\varepsilon_0 c\hbar \simeq 1/137$ is the fine structure constant. If instead of a singular distribution, the bunch has a finite volume, $\pi R_{\mathrm{b}}^2\Delta_z$, and it contains N_{el} electrons, the number of virtual photons associated with this bunch is

$$\frac{N_{\mathrm{ph}}^{(\mathrm{v})}(\gamma\gg 1)}{\alpha_{\mathrm{F}}N_{\mathrm{el}}^2} \simeq \sum_{s=1}^{\infty}\frac{1}{[p_s J_1(p_s)]^2}\frac{J_c^2\left(p_s\frac{R_{\mathrm{b}}}{R_{\mathrm{w}}}\right)}{\sqrt{1+\left(p_s\frac{\gamma\Delta_z}{R_{\mathrm{w}}\pi}\right)^2}} \tag{39}$$

here $J_c(x)\equiv 2J_1(x)/x$. Consequently, a relativistic bunch of 10^{10} electron carries order of 10^{18} virtual photons. The number is weakly dependent on the normalized beam radius and it is roughly proportional to

$$\sim 1/\left(1+10\frac{\gamma\Delta_z}{R_{\mathrm{w}}\pi}\right) \tag{40}$$

(v) Originally, the dielectric function expressed in Eq. (2) was introduced in the homogeneous Maxwell's equation in the context of the linearized laser theory, nevertheless, this constitutive relation is also valid in the non-homogeneous Maxwell equation as long as we maintain the linear regime.

9. Conclusion

We had provided analytic model for Cherenkov wake enhancement in a cylindrical waveguide filled with a CO_2 laser mixture at 10 atm. Geometry of the waveguide is selected such that frequency of one of the wake modes is equal to one of the resonances of the active medium close to 10.6 μm facilitating amplification of this mode by the latter. Due to multiple reflections from the waveguide walls the wake growth rate is enhanced by reciprocal of Cherenkov slippage factor $\overline{\varepsilon}\equiv\varepsilon_{\mathrm{r}}-\beta^{-2}$ of an order of 10^{-3}. A trailing train of electron microbunches located behind the trigger in phase with the enhanced wake will be accelerated by the latter. It is possible in principle to select such charge distribution between the trailing microbunches that will provide gain uniformity for the whole train. A rough assessment is made for saturation limit of the wake growth. For a single resonance of CO_2 this limit is estimated to be of order of 0.5 GeV.

Acknowledgments

This study was supported by the Bi-National Science Foundation. We have benefited from valuable comments from Dr. Patric Muggli.

References

[1] E. Esarey, C. Schroeder, W. Leemans, Rev. Mod. Phys. 81 (2009) 1229.
[2] C. Joshi, Phys. Plasmas 14 (2007) 055501.

[3] C. Joshi, V. Malka, New J. Phys. 12 (2010) 045003.
[4] S. Banna, V. Berezovsky, L. Schachter, Phys. Rev. Lett. 97 (2006) 134801.
[5] W.D. Kimura, et al., Phys. Rev. Lett. 86 (2001) 4041.
[6] M.N. Polyanskiy, I.V. Pogorelsky, V. Yakimenko, Opt. Express 19 (2011) 7717.
[7] D. Haberberger, S. Tochitsky, C. Joshi, Opt. Express 18 (2010) 17865.
[8] J. Miller, A.H. Ross, E. George, Appl. Phys. Lett. 26 (1975) 523.
[9] G.A. Baranov, A.A. Kuchinsky, P.V. Tomashevich, S.M. Kotov, A.V. Vasil'ev, Plasma Devices Oper. 16 (1) (2008) 45.
[10] R.H. Pantell, H.E. Putoff, Fundamentals of Quantum Electronics, Wiley, New York, 1969.
[11] A. Bideau-Mehu, Y. Guern, R. Abjean, A. Johannin-Gilles, Opt. Commun. 9 (1973) 432.
[12] E.R. Peck, B.N. Khanna, J. Opt. Soc. Am. 56 (8) (1966) 1059.
[13] C.R. Mansfield, E.R. Peck, J. Opt. Soc. Am. 59 (2) (1969) 199.
[14] R.W. Fenn, et al., Handbook of Geophysics and the Space Environment, Air Force Geophysics Laboratory, Air Force Systems Command, United States Air Force, 1985.
[15] M. Born, E. Wolf, Principles of Optics, 7th edition, Cambridge University Press, 1999, section 2.3.3.
[16] M. Piestrup, R.A. Powell, G. Rothbart, C.K. Chen, R.H. Pantell, Appl. Phys. Lett. 28 (2) (1976) 92.
[17] A.E. Siegman, Lasers, University Science Books, Sausalito, CA, 1986.
[18] L. Schachter, E. Colby, R. Siemann, Phys. Rev. Lett. 87 (13) (2001) 134802.